

# Hydrolysis, Polymerisation, and Structure of Dimethyltin(IV) in Aqueous Solution. Molecular Structure of the Polymer $[(\text{SnMe}_2)_2(\text{OH})_3]\text{ClO}_4$ †

Takayuki Natsume,<sup>a</sup> Sen-ichi Aizawa,<sup>a</sup> Keiichiro Hatano<sup>b</sup> and Shigenobu Funahashi<sup>\*,a</sup>

<sup>a</sup> Laboratory of Analytical Chemistry, Faculty of Science, Nagoya University, Chikusa, Nagoya 464-01, Japan

<sup>b</sup> Department of Pharmaceutical Sciences, Nagoya City University, Mizuho, Nagoya 467, Japan

The hydrolysis and polymerisation equilibria of dimethyltin(IV) ion have been investigated by potentiometric measurements at 25 °C and  $I = 0.10 \text{ mol dm}^{-3}$  ( $\text{NaNO}_3$ ). Tetramer formation has been observed at high concentrations of dimethyltin(IV) ion up to  $6 \times 10^{-2} \text{ mol dm}^{-3}$ . The polymer structure of  $[(\text{SnMe}_2)_2(\text{OH})_3]\text{ClO}_4$  has been determined by crystal structure analysis: triclinic, space group  $P\bar{1}$ ,  $a = 8.533(1)$ ,  $b = 9.474(1)$ ,  $c = 9.479(2)$  Å,  $\alpha = 88.27(1)$ ,  $\beta = 68.97(1)$ ,  $\gamma = 74.44(1)^\circ$ ,  $Z = 2$ . The final  $R$  value is 0.029. The polymer consists of five-co-ordinate tin(IV) units with di- and mono-hydroxo bridging. The co-ordination geometry of the tin unit is a distorted trigonal bipyramid with two methyl groups and one  $\mu$ -hydroxo group in equatorial positions and the other two  $\mu$ -hydroxo groups in axial positions. The species formed by hydrolysis have been characterised on the basis of the molecular structure in the crystals and are discussed together with their  $\text{p}K_a$  values.

Recently, the significance of organotin chemistry has risen dramatically as a result of the wide range of industrial applications of organotin compounds.<sup>1</sup> From the environmental point of view, the speciation of organotin(IV) species in water is very important in order to understand their reactivities. Therefore, it is necessary to obtain information relating to the hydrolysis and structure of the hydrolysed species.

Though some studies on hydrolysis equilibria of dimethyltin(IV) ion have been reported,<sup>2-5</sup> the detailed features of the polymerisation accompanying hydrolysis are still unclear. The purpose of this work is to clarify more precisely the hydrolysis processes of dimethyltin(IV) as a representative of alkyltin(IV) species and to characterise the polymer species in water. Thus, we report the results of potentiometric measurements of the hydrolysis and the characterisation of the polymer species by crystal structure analysis. The  $\text{p}K_a$  values for dimethyltin(IV) species are also discussed in relation to their structures.

## Experimental

**Reagents.**—Dimethyltin(IV) oxide (Strem) suspended in water was vigorously stirred, and the suspension then filtered. The powder obtained was dissolved in nitric acid (special grade, Wako). The oxide was precipitated by addition of concentrated ammonia (reagent grade, Wako), repeatedly washed with water and dried in a vacuum. These purification procedures were required completely to remove chlorides (Found: C, 14.55; H, 3.60. Calc. for  $\text{C}_2\text{H}_6\text{OSn}$ : C, 14.60; H, 3.65%). Sodium nitrate (reagent grade, Wako), recrystallised twice from water, was used to maintain the ionic strength. Standard sodium hydroxide and nitric acid solutions were prepared from special grade chemicals (Wako).

**Electromotive Force Measurements.**—The potentiometric measurements were carried out using a Metrohm E 654 pH

**Table 1** Experimental conditions for the potentiometric measurements at 25.0 °C and  $I = 0.10 \text{ mol dm}^{-3}$   $[(\text{H,Na})\text{NO}_3]$ \*

$c_{\text{Sn}}^0 / \text{mmol dm}^{-3}$	$c_{\text{HNO}_3}^0 / \text{mmol dm}^{-3}$	$c_{\text{NaOH}}^0 / \text{mol dm}^{-3}$	pH range measured $-\log([\text{H}^+]/\text{mol dm}^{-3})$	Number of data points
1.012	5.038	0.1163	2.5–7.7	50
2.500	5.038	0.1163	2.9–7.7	63
5.013	10.05	0.1163	2.7–7.8	63
10.02	15.08	0.1163	3.1–7.7	67
30.00	40.15	0.1163	3.2–6.2	42
60.02	60.25	0.1041	3.8–5.8	33

\*  $c_{\text{Sn}}^0$ ,  $c_{\text{HNO}_3}^0$  and  $c_{\text{NaOH}}^0$  are the initial concentrations of  $\text{SnMe}_2^{2+}$ ,  $\text{HNO}_3$  and  $\text{NaOH}$  as titrant, respectively.

meter with a hand-piston burette, a glass electrode and a calomel electrode. The electrode couple was standardised by titrating a standard nitric acid solution with a standard sodium hydroxide solution. The determination of the equivalence point by Gran's method allowed us to determine the standard potential  $E^\circ$  and the ionic product of water.<sup>6-9</sup> The temperature of the sample solutions was maintained at  $25.0 \pm 0.1$  °C by circulating thermostatically controlled water through the jacket of a titration vessel. The ionic strength ( $I$ ) was adjusted to  $0.10 \text{ mol dm}^{-3}$  with sodium nitrate. All potentiometric measurements were carried out under a nitrogen atmosphere. The titrations were performed for six different total concentrations of dimethyltin(IV) ion ranging from 1 to  $60 \text{ mmol dm}^{-3}$ . Experimental conditions for the potentiometric titrations are in Table 1. Each experiment was repeated at least twice to confirm reproducibility.

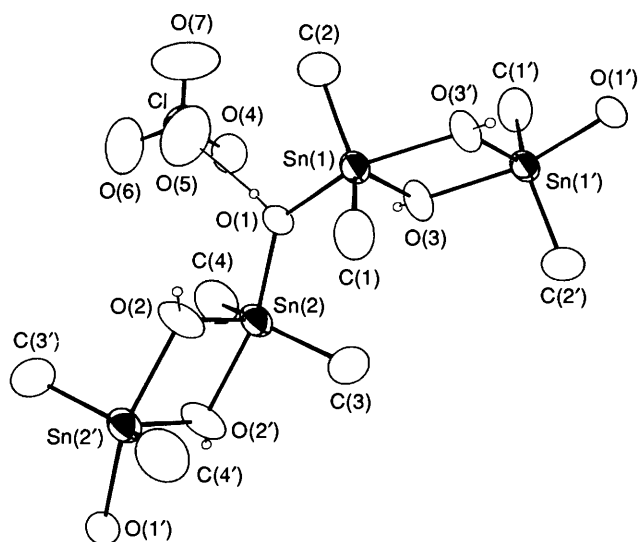
**Preparation of Polymer Crystal.**—To a  $2 \text{ mol dm}^{-3}$  perchloric acid solution ( $20 \text{ cm}^3$ ) containing dimethyltin(IV) oxide (0.66 g,  $4 \text{ mmol}$ ) was added saturated sodium perchlorate solution ( $1 \text{ cm}^3$ ). The pH was adjusted to ca. 4.5 by addition of sodium

† Supplementary data available: see Instructions for Authors, *J. Chem. Soc., Dalton Trans.*, 1994, Issue 1, pp. xxiii–xxviii.

**Table 2** Summary of crystal and intensity collection data for  $[(\text{SnMe}_2)_2(\text{OH})_3]\text{ClO}_4$ 

Formula	$\text{C}_4\text{H}_{15}\text{ClO}_7\text{Sn}_2$
<i>M</i>	448.03
Crystal size/mm	$0.15 \times 0.21 \times 0.42$
Crystal system	Triclinic
Space group	$P\bar{1}$
<i>T</i> /K	293
<i>a</i> /Å	8.533(1)
<i>b</i> /Å	9.474(1)
<i>c</i> /Å	9.479(2)
$\alpha$ /°	88.27(1)
$\beta$ /°	68.97(1)
$\gamma$ /°	74.44(1)
<i>U</i> /Å <sup>3</sup>	687(3)
<i>Z</i>	2
<i>D<sub>c</sub></i> /g cm <sup>-3</sup>	2.164
$\mu$ /cm <sup>-1</sup>	38.5
<i>F</i> (000)	424
$2\theta$ range/°	4–55
Scan technique	$\omega$ -2 $\theta$
Scan range/ $\omega$	$0.65 + 0.35 \tan \theta$
No. of unique observed data	2912
$[F_o > 3\sigma(F_o)]$	
<i>R</i> <sup>a</sup>	0.029
<i>R</i> <sup>b</sup>	0.030
No. of variables	128

<sup>a</sup>  $\sum ||F_o| - |F_c|| / \sum |F_o|$ . <sup>b</sup>  $[\sum w(|F_o| - |F_c|)^2 / \sum w(F_o)^2]^{1/2}$  with unit weights.

**Fig. 1** An ORTEP<sup>12</sup> diagram of the polymer of  $[(\text{SnMe}_2)_2(\text{OH})_3]\text{ClO}_4$  showing the atom-labelling scheme. All hydrogen atoms have been omitted

hydroxide solution. Slow evaporation of the solution for some weeks resulted in crystals suitable for X-ray analysis {Found: C, 10.65; H, 3.45. Calc. for  $[(\text{SnMe}_2)_2(\text{OH})_3]\text{ClO}_4$ : C, 10.70; H, 3.35%}.

**Crystal Structure Analysis.**—A rhombic crystal of the perchlorate salt obtained as above was examined on an Enraf-Nonius CAD4 Kapp diffractometer equipped with graphite-monochromated Mo-K $\alpha$  radiation ( $\lambda = 0.71073$  Å). Least-squares refinement of the setting angles of 25 reflections, collected in the range  $20 < 2\theta < 27^\circ$ , led to the cell constants. Table 2 gives a summary of the crystal data and intensity-collection parameters. The intensity data were corrected for the standard Lorentz and polarisation effects. An empirical absorption correction was applied.

**Table 3** Atomic coordinates with estimated standard deviations (e.s.d.s) in parentheses

Atom	x	y	z
Sn(1)	0.709 05(4)	0.380 28(3)	0.952 78(3)
Sn(2)	0.799 36(4)	0.062 37(4)	0.648 94(4)
Cl	0.239 0(2)	0.161 3(2)	0.857 0(2)
O(1)	0.773 6(4)	0.160 5(3)	0.858 6(3)
O(2)	1.057 5(4)	0.039 3(5)	0.588 1(4)
O(3)	0.465 6(4)	0.396 7(3)	0.956 7(3)
O(4)	0.400 2(5)	0.139 9(5)	0.878 5(5)
O(5)	0.147 2(6)	0.065 4(6)	0.938 6(7)
O(6)	0.137 4(7)	0.308 5(6)	0.915 4(8)
O(7)	0.266 0(7)	0.145 2(8)	0.704 9(6)
C(1)	0.859 8(8)	0.461 6(6)	0.757 9(7)
C(2)	0.730 5(8)	0.324 7(8)	1.163 0(6)
C(3)	0.673 3(8)	0.251 9(7)	0.567 7(7)
C(4)	0.738 5(9)	-0.132 1(7)	0.725 9(8)

**Table 4** Bond lengths (Å) and angles (°) with e.s.d.s in parentheses

Sn(1)–O(1)	2.139(3)	Sn(2)–O(2')	2.236(3)
Sn(1)–O(3)	2.030(4)	Sn(2)–C(3)	2.111(7)
Sn(1)–O(3')	2.220(3)	Sn(2)–C(4)	2.088(7)
Sn(1)–C(1)	2.099(6)	Cl–O(4)	1.424(5)
Sn(1)–C(2)	2.105(7)	Cl–O(5)	1.394(6)
Sn(2)–O(1)	2.132(3)	Cl–O(6)	1.433(6)
Sn(2)–O(2)	2.019(4)	Cl–O(7)	1.382(6)
O(1)–Sn(1)–O(3)	85.4(1)	O(2)–Sn(2)–O(2')	69.9(2)
O(1)–Sn(1)–O(3')	155.1(1)	O(2)–Sn(2)–C(3)	112.2(2)
O(1)–Sn(1)–C(1)	96.9(2)	O(2)–Sn(2)–C(4)	111.0(2)
O(1)–Sn(1)–C(2)	96.8(2)	O(2')–Sn(2)–C(3)	90.3(2)
O(3)–Sn(1)–O(3')	69.7(1)	O(2')–Sn(2)–C(4)	91.6(2)
O(3)–Sn(1)–C(1)	112.2(2)	C(3)–Sn(2)–C(4)	134.5(3)
O(3)–Sn(1)–C(2)	111.5(2)	O(4)–Cl–O(5)	111.0(3)
O(3')–Sn(1)–C(1)	92.1(2)	O(4)–Cl–O(6)	106.7(4)
O(3')–Sn(1)–C(2)	93.2(2)	O(4)–Cl–O(7)	110.9(3)
C(1)–Sn(1)–C(2)	135.0(3)	O(5)–Cl–O(6)	108.1(3)
O(1)–Sn(2)–O(2)	85.8(1)	O(5)–Cl–O(7)	110.6(5)
O(1)–Sn(2)–O(2')	155.5(1)	O(6)–Cl–O(7)	109.3(4)
O(1)–Sn(2)–C(3)	97.9(2)	Sn(1)–O(1)–Sn(2)	135.5(2)
O(1)–Sn(2)–C(4)	98.9(2)		

The structure was solved by heavy-atom methods<sup>10</sup> and refined by Fourier-difference and full-matrix least-squares techniques.<sup>10</sup> All non-hydrogen atoms were refined with anisotropic thermal parameters. The hydrogen atoms bound to oxygen were found in a Fourier map and those bound to carbon were included in calculated positions. All hydrogen parameters were treated as fixed values. Atomic scattering factors were taken from ref. 11.

Additional material available from the Cambridge Crystallographic Data Centre comprises H-atom coordinates and thermal parameters.

## Results and Discussion

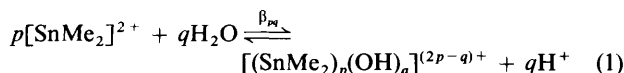
**Structure of Polymer of  $[(\text{SnMe}_2)_2(\text{OH})_3]\text{ClO}_4$ .**—A perspective view of a centrosymmetric polymer unit,  $[(\text{SnMe}_2)_2(\text{OH})_3]\text{ClO}_4$ , is displayed in Fig. 1 with the labelling employed for the atoms of an asymmetric unit. Atomic coordinates are listed in Table 3; selected bond lengths and angles in Table 4.

The polymer structure consists of five-co-ordinate tin(IV) units with di- and mono-hydroxo bridging. The co-ordination geometry of the tin unit is a distorted trigonal bipyramid with two methyl groups and one  $\mu$ -hydroxo group in equatorial positions and the other two  $\mu$ -hydroxo groups in axial positions. Each di- $\mu$ -hydroxo bridge has two different Sn–O bond lengths, 2.030 and 2.220 Å for Sn(1)–O(3) and Sn(1)–O(3') and 2.019 and 2.236 Å for Sn(2)–O(2) and Sn(2)–O(2'), respectively. The shorter and longer bonds correspond to the

equatorial (Sn–O<sub>eq</sub>) and axial bonds (Sn–O<sub>ax</sub>), respectively. This di- $\mu$ -hydroxo structure is quite similar to that of the nitrate dimer, di- $\mu$ -hydroxo-bis(dimethylnitratotin),<sup>13</sup> in which the two bridging bond lengths are 2.06 and 2.18 Å. On the other hand, the mono- $\mu$ -hydroxo oxygen O(1) bridges two tin atoms, Sn(1) and Sn(2), *via* their axial positions, with similar bond lengths, 2.139 and 2.132 Å, respectively. These Sn(1)–O(1) and Sn(2)–O(1) axial bonds are notably shorter than Sn–O<sub>ax</sub> in the di- $\mu$ -hydroxo bridging. This reveals that the electron density is localised in Sn–O<sub>eq</sub>, and consequently Sn–O<sub>ax</sub> is elongated in the di- $\mu$ -hydroxo bridging. Thus the covalency increases in the following order: Sn–O<sub>ax</sub> in di- $\mu$ -hydroxo bridging [Sn(1)–O(3') and Sn(2)–O(2')] < Sn–O in mono- $\mu$ -hydroxo bridging [Sn(1)–O(1) and Sn(2)–O(1)] < Sn–O<sub>eq</sub> in di- $\mu$ -hydroxo bridging [Sn(1)–O(3) and Sn(2)–O(2)].

Though the central tin atom and three equatorially coordinated atoms are almost coplanar, the C–Sn–C angles are substantially greater than 120° [C(1)–Sn(1)–C(2) 135.0 and C(3)–Sn(2)–C(4) 134.5°]. Furthermore, the O–Sn–O axial axis is largely bent toward the equatorial oxygen atom [O(1)–Sn(1)–O(3') 155.1 and O(1)–Sn(2)–O(2') 155.5°]. Such distortion has been similarly observed in the nitrate dimer (C<sub>eq</sub>–Sn–C<sub>eq</sub> 139.9 and O<sub>ax</sub>–Sn–O<sub>ax</sub> 149.3°).<sup>13</sup> Since Sn–C bonds are more covalent than Sn–O bonds, the increase in the C–Sn–C angle and decrease in the O–Sn–O angle reduce the electronic repulsion, and the increase in linearity of the C–Sn–C skeleton enhances the *s* character in the sp<sup>2</sup> hybridisation of the three equatorial bonds, which is consistent with the tendency to maximise the *s* character in the hybrid orbital of the tin atom.<sup>14,15</sup>

**Stability Constants and Structures of Hydrolysed Dimethyltin(IV) Species in Solution.**—Dimethyltin(IV) ion hydrolyses to form a series of mono- and poly-nuclear hydroxo species and precipitates at high pH and concentration. The hydrolysis can be expressed by equation (1) where  $\beta_{pq}$  is the overall



stability constant defined as  $[(\text{SnMe}_2)_p(\text{OH})_q]^{(2p-q)+} [\text{H}^+]^q / [\text{SnMe}_2^{2+}]^p$ .

The stability constants were evaluated using the computer program SUPERQUAD.<sup>16</sup> First we took the following 18 species into consideration: (1, *q*), *q* = 0–3; (2, *q*), *q* = 1–4; (3, *q*), *q* = 1–4; (4, *q*), *q* = 1–6; where (*p*, *q*) represents  $[(\text{SnMe}_2)_p(\text{OH})_q]^{(2p-q)+}$ . By using several different combinations of the data for six different concentrations of SnMe<sub>2</sub><sup>2+</sup>, from 1 to 60 mmol dm<sup>-3</sup> (see Table 1), the species (1,3), (2,1), (3,1), (3,3), (3,4), (4,1), (4,2), (4,3) and (4,4) were rejected by the criteria of SUPERQUAD. The rejection of (3,1), (4,1) and (4,2) is reasonable because of the lack of hydroxo groups to form the corresponding polymerised species, and the absence of (2,1), (3,3), (4,3) and (4,4) is in accord with previous results.<sup>4,5</sup> We should note, in contrast to that work,<sup>4,5</sup> the formation of species (1,3) and (3,4) was not confirmed, but the presence of (3,2), (4,5) and (4,6) was observed. The absence of the (1,3) species is due to precipitation in the high pH region. On the other hand, the tetramers (4,5) and (4,6) should appear only at high concentration of SnMe<sub>2</sub><sup>2+</sup> as employed in the present work. Furthermore, the existence of (3,2) and (3,4) was checked using only the data for high concentrations. This confirmed the rejection of (3,4) and the existence of (3,2) at very low pH (see Fig. 2).

Finally, the computation using all the 318 data points for the six different concentrations (Table 1) led to the same result and we concluded that species (1,1), (1,2), (2,2), (2,3), (2,4), (3,2), (4,5) and (4,6) exist under our experimental conditions. Their stability constants are summarised in Table 5 together with some literature values.<sup>3–5</sup> Fig. 2 shows the species distribution diagrams for the lowest and highest tin concentrations under our experimental conditions.

**Table 5** Stability constants of hydrolysed dimethyltin(IV) species at 25.0 °C and 0.10 mol dm<sup>-3</sup> [(H,Na)NO<sub>3</sub>]

<i>(p, q)</i>	log $\beta_{pq}$			
	<i>a</i>	<i>b</i>	<i>c</i>	<i>d</i>
(1,1)	-3.176(4)	-3.124	-3.251	-3.2
(1,2)	-8.423(3)	-8.428	-8.535	
(1,3)		-19.450		
(2,2)	-4.687(14)	-5.05	-5.05	-4.6
(2,3)	-9.644(12)	-9.74	-9.81	
(2,4)	-15.443(21)			
(3,2)	-3.205(53)			
(3,4)			-11.52	
(4,5)	-11.724(26)			
(4,6)	-16.365(20)	-16.30		

<sup>a</sup> This work. <sup>b</sup> Ref. 5, *I* = 0.1 mol dm<sup>-3</sup> (KNO<sub>3</sub>). <sup>c</sup> Ref. 4, *I* = 0.1 mol dm<sup>-3</sup> (NaCl). <sup>d</sup> Ref. 3, *I* = 0.1 mol dm<sup>-3</sup> (KNO<sub>3</sub>).

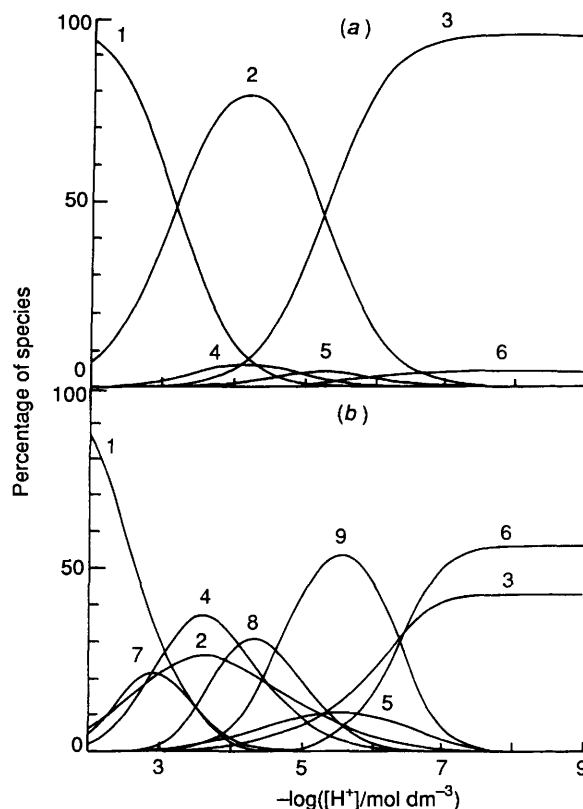


**Fig. 2** Distribution diagrams of hydrolysed dimethyltin(IV) species as a function of  $-\log[\text{H}^+]$ :  $c_{\text{Sn}}/\text{mol dm}^{-3} = 1.012 \times 10^{-3}$  (a) and  $6.002 \times 10^{-2}$  (b). (*p, q*) =  $[(\text{SnMe}_2)_p(\text{OH})_q]^{(2p-q)+}$ ; 1, (1,0); 2, (1,1); 3, (1,2); 4, (2,2); 5, (2,3); 6, (2,4); 7, (3,2); 8, (4,5); 9, (4,6)

It has been shown that the aquadimethyltin(IV) ion, (1,0), has an octahedral geometry with a linear C–Sn–C skeleton and four water molecules in equatorial positions bound essentially by ion–dipole attraction.<sup>15</sup> Transfer of a proton from a coordinated water will result in a strengthening of an Sn–O bond to a hydroxo group and weakening of those to aqua groups because of the difference in the donor strength of hydroxo and aqua groups. The formation of a stronger Sn–OH bond will direct the *s* character of the two Sn–C bonds towards the Sn–OH bond, and consequently the C–Sn–C angle will decrease appreciably. Such a tendency has been observed in the Raman spectra.<sup>15</sup> Thus, water molecules in species (1,1) can be attached by the ion–dipole interaction at both sides of the distorted trigonal plane containing the two Sn–C bonds and an Sn–OH bond, forming a distorted trigonal-bipyramidal

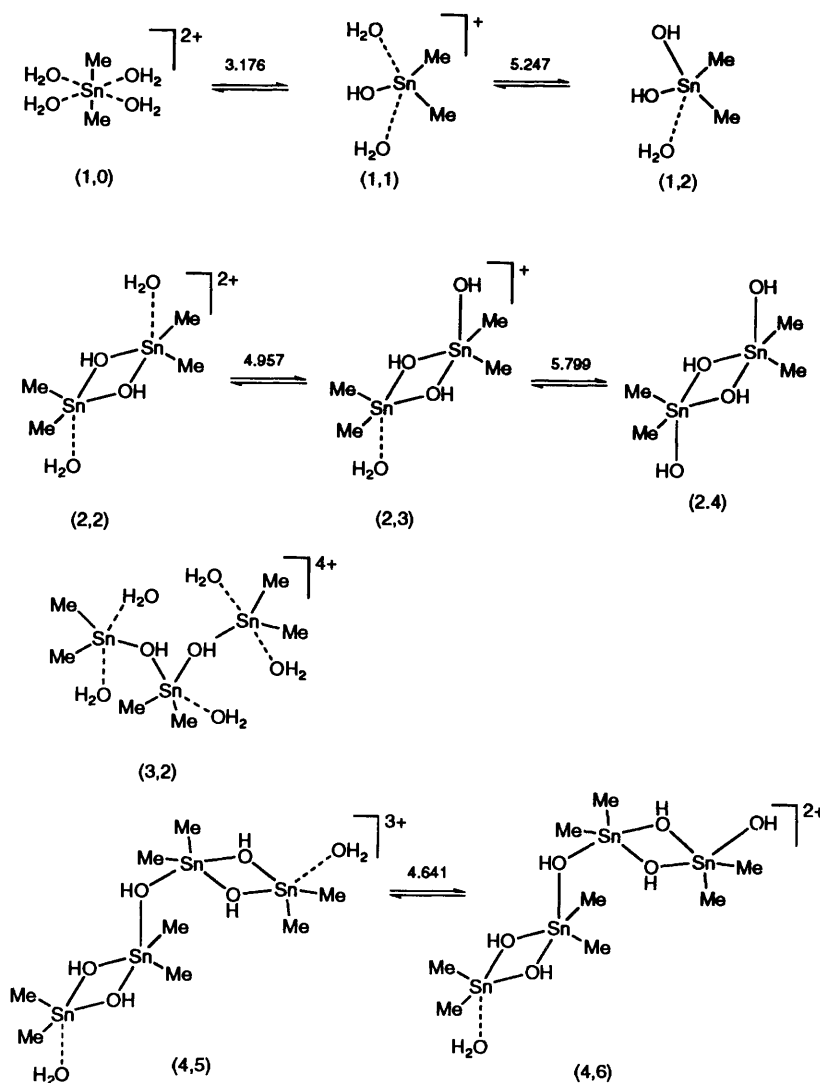


Fig. 3 Plausible structures of the dimethyltin(IV) species in aqueous solution. The corresponding  $pK_a$  values are given where  $pK_a = -\log [H^+][p,q-1][p,q]^{-1}$

structure. This geometry is virtually the same as that of the tin(IV) unit in the crystals.

A tetrahedral geometry has been suggested for dimethyltin dihydroxide, (1,2).<sup>17</sup> However, there is a possibility that a water molecule is weakly bound to the central tin atom, because the electronegativity of the oxygen in co-ordinated hydroxo groups induces localisation of the positive charge in the tin(IV) centre. This possibility is supported by the crystal structure of dimethyldinitratotin(IV) in which two formally neutral oxygens of the nitrate ligands are weakly co-ordinated to the distorted-tetrahedral tin(IV) core.<sup>18</sup>

It is likely that the polymerised structures of the dimethyltin(IV) species in aqueous solution comprise a five-co-ordinate tin(IV) unit as observed in the crystal of the polymer. Plausible structures for all the dimethyltin(IV) species in aqueous solution as indicated by the potentiometric measurements are shown schematically with their  $pK_a$  values in Fig. 3.

An increase in electron density at tin is one of the most important ways of reducing the acidity of dimethyltin(IV) species. Therefore, the acidity should depend on the number of hydroxo groups bound to each tin(IV) unit because of the difference in donicity of hydroxo and aqua groups. For the monomer, the  $pK_a$  value of (1,1) with one hydroxo group is much greater than that of (1,0) with no hydroxo group (see  $pK_a$  values in Fig. 3). Though the monoaquadimethyltin(IV) unit hydrolyses to give the dimers (2,2) and (2,3), the neighbouring

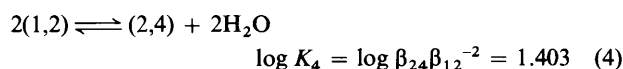
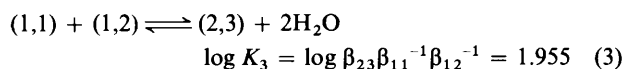
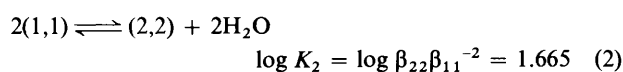
tin(IV) unit linked by di- $\mu$ -hydroxo bridging in each species contains no and one non-bridging hydroxo group, respectively. Therefore, the tin atom in the monoaquadimethyltin(IV) unit of (2,3) is more electron rich than those of (2,2) and, in fact, (2,3) is less acidic than is (2,2). Although the number of hydroxo groups per tin(IV) unit in (1,1) and (2,2) is the same, unity, the delocalisation of electron density through  $\mu$ -hydroxo bridging facilitates hydrolysis of species (2,2) and reduces its  $pK_a$  value compared with that of (1,1).

In addition to the electron density, a slight change in geometry of the tin(IV) unit can affect the bond strength significantly. It is likely that a dimethyltin(IV) unit with two  $\mu$ -hydroxo groups possesses four covalent bonds in which the hybridisation of the tin atom is regarded as  $sp^3$ , although an aqua group may also be bound by dipole interaction leading to a distorted trigonal-bipyramidal structure. On the other hand, the hybridisation of the tin atom in a dimethyltin(IV) unit with three  $\mu$ -hydroxo groups is formally considered to be  $sp^2$  because a large d-s orbital separation renders  $sp^3d$  hybridisation unlikely.<sup>15,19</sup> Therefore, the two axial Sn-OH bonds in the trihydroxo unit are more ionic and longer and the equatorial Sn-OH bond is more covalent and shorter than those in the dihydroxo unit. This tendency is consistent with the slight difference in structure between the polymer of  $[(SnMe_2)_2(OH)_3]ClO_4$  with three  $\mu$ -hydroxo groups in each unit and the nitrate dimer with two  $\mu$ -hydroxo groups and the more ionic

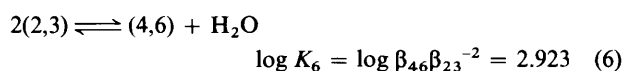
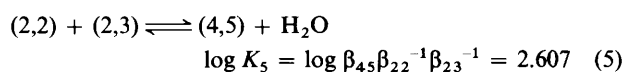
nitrate oxygen in each unit,<sup>13</sup> as described above. The Sn–O<sub>ax</sub> and Sn–O<sub>eq</sub> bonds of the di- $\mu$ -hydroxo bridge in the polymer are longer and shorter than corresponding bonds in the dimer, respectively. Furthermore, the C–Sn–C angle in the polymer is a little larger than that in the dimer. The structure of the tin(IV) unit can influence that of the neighbouring unit, *i.e.* shortening of the Sn–O<sub>eq</sub> bond and elongation of the Sn–O<sub>ax</sub> bond in the di- $\mu$ -hydroxo bridge result in elongation of the Sn–O<sub>ax</sub> bond and shortening of the Sn–O<sub>eq</sub> bond in the neighbouring unit because of the localisation of electron density through the  $\mu$ -hydroxo bridge, and consequently induce sp<sup>2</sup> character in the neighbouring tin(IV) centre.

Since each tin(IV) unit in species (2,2) contains two  $\mu$ -hydroxo groups, both tin centres have sp<sup>3</sup> character. On the other hand, sp<sup>2</sup> character is induced in the tin(IV) centre of the terminal unit in (4,5) because the neighbouring middle units have three  $\mu$ -hydroxo groups. This sp<sup>2</sup> character facilitates the formation of another covalent bond, even if the average electron density per tin(IV) centre in (4,5) is higher than that in (2,2). The difference in pK<sub>a</sub> between (4,5) and (2,2) may reflect the slight difference in structure.

As is apparent from Fig. 2, the formation of species (2,2) and (2,4) is promoted in the pH region where (1,1) and (1,2) exist, respectively, by increasing c<sub>Sn</sub>. Similarly, (2,3) is formed in the pH region where (1,1) and (1,2) co-exist. The dimerisation equilibria with the corresponding equilibrium constants at 25 °C are shown in equations (2)–(4). The equilibrium constants



for the tetramer formation are as given in equations (5) and (6).



It is obvious that the polymerisation is stabilised by  $\mu$ -hydroxo bridging. Interestingly, the stabilisation upon dimer formation

( $\Delta G^\circ = -11.2$  to  $-8.0$  kJ mol<sup>-1</sup> at 25 °C) corresponding to di- $\mu$ -hydroxo linkage formation is smaller than that upon tetramer formation ( $\Delta G^\circ = -16.7$  to  $-14.9$  kJ mol<sup>-1</sup> at 25 °C) corresponding to  $\mu$ -hydroxo bridging. This finding indicates that the rigidity of the di- $\mu$ -hydroxo linkage is more entropically unfavoured than is the mono- $\mu$ -hydroxo bridge, although dimer formation [equations (2)–(4)] results in the loss of two co-ordinated water molecules while tetramer formation [equations (5) and (6)] involves the loss of one. The stabilisation upon mono- $\mu$ -hydroxo bridging allows us to predict that more highly polymerised species form at higher concentrations of dimethyltin(IV) ion, as observed in the crystal.

### Acknowledgements

This work was supported by a Grant-in-Aid for Scientific Research (No. 04403011) from the Ministry of Education, Science, and Culture of Japan. S. A. gratefully acknowledges receipt of a grant from the Kurata Foundation.

### References

- 1 I. Omae, *Organotin Chemistry*, Elsevier, Amsterdam, 1989, pp. 1–9.
- 2 R. S. Tobias, I. Ogrins and B. A. Nevett, *Inorg. Chem.*, 1962, **1**, 639.
- 3 M. Yasuda and R. S. Tobias, *Inorg. Chem.*, 1963, **2**, 207.
- 4 R. S. Tobias and M. Yasuda, *Can. J. Chem.*, 1964, **42**, 781.
- 5 G. Arena, R. Purrello, E. Rizzarelli, A. Gianguzza, L. Pellerito and S. Musumeci, *J. Chem. Soc., Dalton Trans.*, 1989, 773.
- 6 G. Gran, *Analyst (London)*, 1952, **77**, 661.
- 7 F. J. A. Rossotti and H. Rossotti, *J. Chem. Educ.*, 1965, **42**, 375.
- 8 J. A. Bojani, *J. Chem. Educ.*, 1986, **63**, 724.
- 9 H. S. Dunsmore and D. Midgley, *Anal. Chim. Acta*, 1972, **61**, 115.
- 10 SDP Structure Determination Package, Enraf–Nonius, Delft, 1985.
- 11 *International Tables for X-Ray Crystallography*, Kynoch Press, Birmingham, 1974, vol. 4.
- 12 C. K. Johnson, ORTEP, Report ORNL-5138, Oak Ridge National Laboratory, Oak Ridge, TN, 1976.
- 13 A. M. Domingos and G. M. Sheldrick, *J. Chem. Soc., Dalton Trans.*, 1974, 475.
- 14 H. A. Bent, *J. Inorg. Nucl. Chem.*, 1961, **19**, 43.
- 15 M. M. McGrady and R. S. Tobias, *Inorg. Chem.*, 1964, **3**, 1157.
- 16 P. Gans, A. Sabatini and A. Vacca, *J. Chem. Soc., Dalton Trans.*, 1985, 1195.
- 17 R. S. Tobias and C. E. Freidline, *Inorg. Chem.*, 1965, **4**, 215.
- 18 J. Hilton, E. K. Nunn and S. C. Wallwork, *J. Chem. Soc., Dalton Trans.*, 1973, 173.
- 19 M. M. McGrady and R. S. Tobias, *J. Am. Chem. Soc.*, 1965, **87**, 1909.

Received 17th March 1994; Paper 4/01613K